THERMOCOAX rhodium SPND sensitivity dispersion and validation of the sensitivity calculation model

L. Vermeeren[1] *, W. Leysen[1], L. Pichon[2], V. Salou[2] and G. Helleux[2]
[1] SCK•CEN
[2] THERMOCOAX
* lvermeer@sckcen.be

Abstract— **This paper describes the neutron irradiation tests of 7 THERMOCOAX Self-Powered Neutron detectors (SPNDs) in the BR1 reactor at SCK•CEN. The SPNDs were fabricated according to the same specifications, but from different fabrication batches. The SPND signals were recorded during stepwise power-up of the reactor, proving the linearity of the SPND response within a wide thermal neutron flux range: from as low as $0.8 \cdot 10^9$ n/(cm s) to $2.6 \cdot 10^{11}$ n/(cm s). Intercomparison of the SPND signals shows a very small spread, confirming the repeatability of the THERMOCOAX fabrication processes. The overall neutron sensitivities of the seven SPNDs agreed within a 1% margin.**
The experimental data were analyzed in terms of prompt and various delayed responses. Prompt contributions to the signal are due to external gamma induced processes and to processes involving gamma rays emitted instantaneously upon neutron capture. The main contribution in a rhodium SPND is due to activation of the rhodium emitter and beta emission during decay of the activated rhodium and leads to a delayed response with a characteristic time of a few minutes. Activation and subsequent beta decay in other materials present in the SPND lead to additional minor delayed signal contributions. The partial SPND sensitivities due to all these processes were calculated using an MCNPX based model and were compared with experimental sensitivities based on the recorded data. The results were in fair agreement; for the overall SPND neutron sensitivity an agreement within a 1% margin was achieved.

***Keywords*—Nuclear measurements, neutron detectors, reactor instrumentation, modelling**

I. Introduction

A crucial parameter in the monitoring of the behavior of research reactors and power reactors is the neutron flux distribution within the reactor core. Fission chambers can provide instantaneous data on in-core reactor neutron flux measurements. But thanks to improved simulation tools, there is a growing interest in self-powered neutron detectors (SPNDs) as a valuable and cheaper alternative for fission chambers for thermal neutron flux monitoring. They can be implemented as fixed in-core sensors for applications in which mobile in-core systems are not acceptable and in which ex-core sensors cannot ensure all required functions [1].

This paper deals with the characterization of SPNDs with rhodium emitter, fabricated by THERMOCOAX. A set of seven SPNDs was tested in the BR1 reactor at SCK•CEN. All SPNDs were fabricated according to the same specifications (see Fig. 1): a 250 mm long, 0.50 mm diameter rhodium emitter, surrounded by a 0.185 mm thick alumina insulator and enclosed in a 0.245 mm thick SS316L sheath (outer diameter 1.36 mm). The emitters parts of the SPNDs were integrated without external welds in 1.36 mm diameter twin core cables, with two 0.21 mm diameter SS316L core wires. The seven SPNDs were taken from different fabrication batches.

A first goal of the test was to investigate the linearity and the spread in neutron sensitivity of the SPND in order to realize a complete characterization in terms of linearity, sensitivity repeatability and deviation. Secondly, the experimental sensitivities were also compared with results from detailed Monte Carlo modelling of the various contributions to the SPND signal in order to validate the calculation approach.

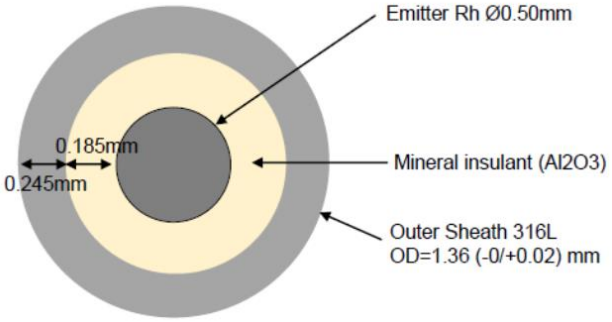

Fig. 1. Cross section of the sensitive part of the SPNDs with indication of the dimensions

II. Experimental set-up

The SPNDs were irradiated in the Y7 channel of the BR1 reactor (see Figure 2). BR1 is an air cooled graphite moderated thermal reactor with a nominal thermal power of 700 kW; for short periods the power can be raised to 1 MW. An activation dosimetry campaign performed just before the test irradiations discussed here, yielded an unperturbed conventional thermal neutron flux of $1.80 \cdot 10^{11}$ n/(cm /s) at a nominal BR1 power of 700 kW. The SPNDs were positioned with the emitters centered at the reactor mid-plane (so 12.5 cm emitter length at each side of the mid-plane). So the SPND emitters are fully exposed to the maximum flux (less than 1 % flux gradient over the emitter length).

L. Vermeeren and W Leysen are with the Nuclear Research Centre SCK•CEN, B-2400, Mol, Belgium (e-mail: lvermeer@sckcen.be); L. Pichon, V. Salou and G. Helleux are with Thermocoax, 8 Rue du Pré Neuf, 61100 St Georges des Groseillers, France

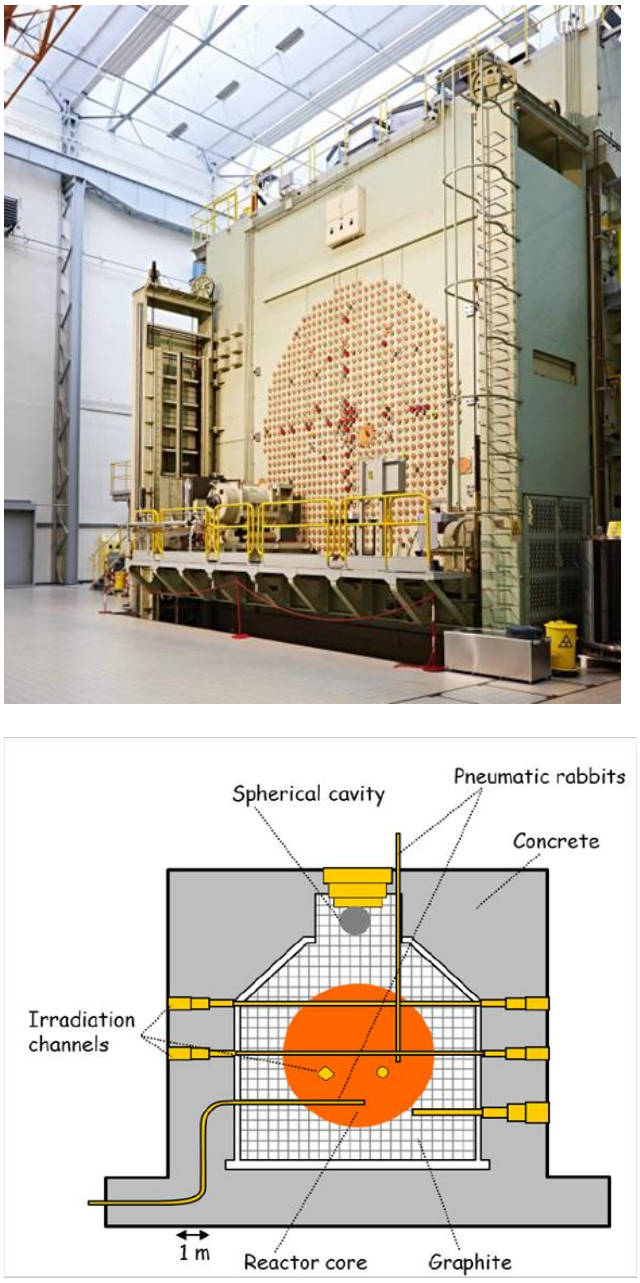

Fig. 2. Picture of the BR1 reactor (top) and schematic cross section of the BR1 (bottom); the SPNDs were loaded in the Y7 channel, which is a horizontal channel perpendicular to the plane of this sketch (indicated as a yellow square) and parallel with the reactor fuel.

The neutron and the gamma spectra in channel Y7 as calculated by means of MCNP [2] are shown in Figs. 3 and 4. At a nominal BR1 power of 700 kW, a total neutron flux of $4.06 \cdot 10^{11}$ n/(cm s) was obtained and a conventional neutron flux of $1.81 \cdot 10^{11}$ n/(cm s), in very good agreement with the dosimetry results; the total gamma flux is $5.43 \cdot 10^{10}$ γ(/cm s). These spectra were used for all partial SPND sensitivity calculations.

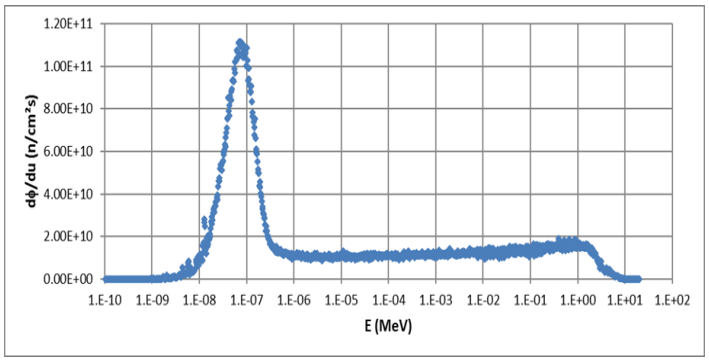

Fig. 3 – Calculated neutron spectrum in BR1/Y7. The data are represented as absolute flux values (at nominal BR1 power of 700 kW) per unit lethargy; this means that the total flux can be obtained directly via the surface under the curve.

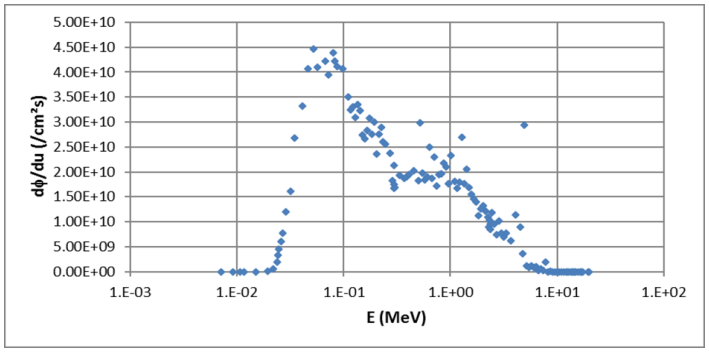

Fig. 4 – Calculated gamma spectrum in BR1/Y7 (also formally represented as absolute flux values per unit lethargy for 700 kW reactor power)

Figure 5 shows a few pictures of the SPND holder. The seven SPNDs are placed on fixed distance from the center of the aluminum box (where a thermocouple was positioned). They were guided through 1.5 mm holes in two thin aluminum plates (at both ends of the emitter part). At the exit of the box, the cables were strapped together to avoid any axial movement during manipulations. The cables were guided further through the long aluminum tube and through the shielding chicane at the border of the reactor. The acquisition system (connection box with 1 MΩ resistances, Keysight multimeter (34972A) with scanner cards (34902A) and pc) was positioned next to the reactor.

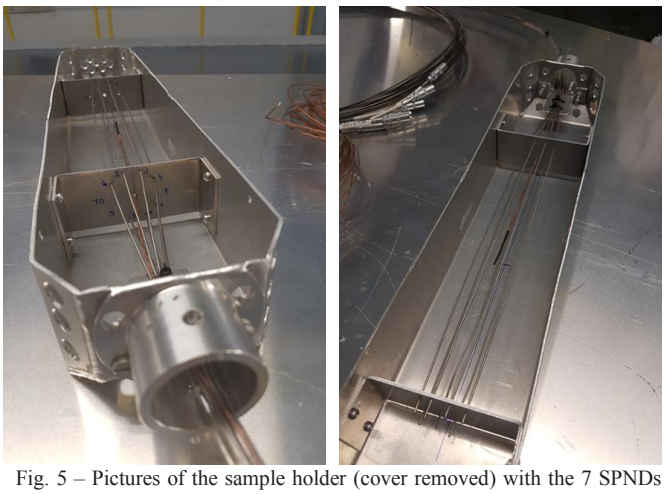

Fig. 5 – Pictures of the sample holder (cover removed) with the 7 SPNDs and a thermocouple

III. SPND SIGNAL COMPONENTS

The SPND current is composed of various components. For a rhodium SPND, the major component is due to neutron capture by the rhodium nuclei (^{103}Rh) in the emitter. Neutron capture by ^{103}Rh leads to the formation of ^{104}Rh in two different states: the excited state ^{104m}Rh, that decays with a half-life of 4.4 minutes to the ground state, or immediately the ground state ^{104}Rh, which decays with a half-life of 42 seconds towards (stable) ^{104}Pd.

The de-excitation from ^{104m}Rh to ^{104}Rh occurs mainly via internal transition, which will lead to a negligible signal contribution. Ultimately, all activated rhodium nuclei will decay towards ^{104}Pd, during which a beta ray is emitted, as well as some gamma rays. This beta (actually a fast electron) has a significant probability to escape from the emitter and reach the collector after crossing the insulator. This corresponds to a charge transfer from emitter to collector, which can be measured as a current when externally closing the circuit (with an ampere meter). This component has a delayed character related to the half-lifes of ^{104m}Rh and ^{104}Rh.

The neutron capture also leads to a signal component with a prompt character. This component results from the gammas emitted instantaneously during neutron capture. Interaction of these gammas with electrons (photoelectric effect, Compton scattering, pair formation,…) can lead to sufficiently energetic electrons so that they can cross the insulator and contribute to the current. Since this is a two-step process (neutron interaction + gamma-electron interaction), the resulting current is typically an order of magnitude lower than the beta induced current.

Neutron capture in other parts of the SPND (insulator and sheath) and in the materials surrounding the SPND can lead to additional (usually minor) contributions to the detector signal.

Similarly, external gammas can interact with electrons in the SPND (and its surroundings) and generate a current. It is known that this current contribution depends strongly on the materials and the geometry of the surroundings.

IV. MCSS MODELLING

All relevant signal contributions were calculated according to the MCSS model described in [3] and using the spectra from Figs. 3 and 4:

- the main rhodium beta related contribution
- aluminum beta contribution (from the insulator)
- manganese beta contribution (1.74% mass fraction in the sheath material)
- prompt neutron contribution
- gamma contribution

All related MCNPX calculations were performed for an infinitely long geometry (results per cm length), which included the seven SPNDs and the aluminum box (9.6 cm * 9.6 cm; wall thickness 0.2 cm). The neutron (or gamma) source was defined on a cylindrical surface at radius 6.9 cm in order to cover the complete geometry. The results for all seven SPNDs were identical within the statistical uncertainties, so average values were taken.

The calculations lead to the following partial SPND currents (at 700 kW reference reactor power):

- due to Rh betas : 5.18 nA (94.4%)
- due to Al betas : 0.0050 nA (0.1%)
- due to Mn betas : -0.0095 nA (-0.2%)
- prompt neutron contribution : 0.29 nA (5.3%)
- prompt gamma contribution : 0.023 nA (0.4%)
- total prompt contribution : 0.31 nA (5.6%)
- total SPND current: 5.49 nA (100%)

V. EXPERIMENTAL DATA ANALYSIS

A. *Example of experimental data*

Emitter and compensator current data were recorded sequentially for all seven SPNDs (1 complete data set every 20 seconds) during stepwise BR1 power increase (3-10-30-100-200-400-600-800-1000 kW) followed by a power reduction to 300 kW and scram (see Fig. 6). The power range [3-1000 kW] corresponds to a conventional thermal neutron flux range of [$8\cdot10^{8}$ - $2.6\cdot10^{11}$ n/(cm s)].

Additionally, in order to test the prompt response fraction and the repeatability, three tests at 300 kW reactor power were performed with continuous measurement of the SPND1 differential current (one point each 400 ms) (see Fig. 7).

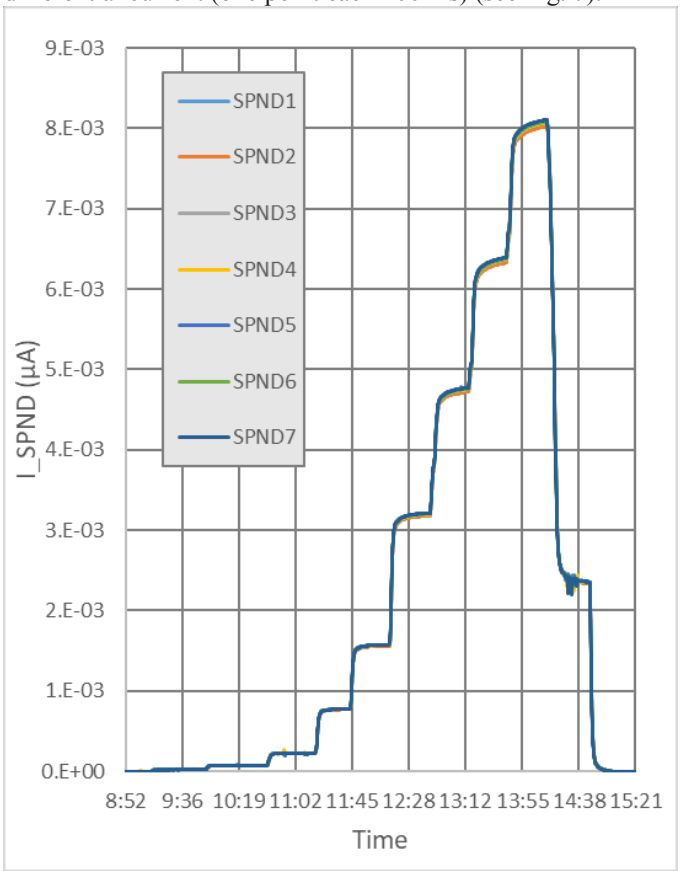

Fig. 6 – Raw differential signals (emitter minus compensator) of the seven SPNDs during stepwise BR1 power increase and scram. The signals are so close to each other that they can hardly be distinguished in this representation.

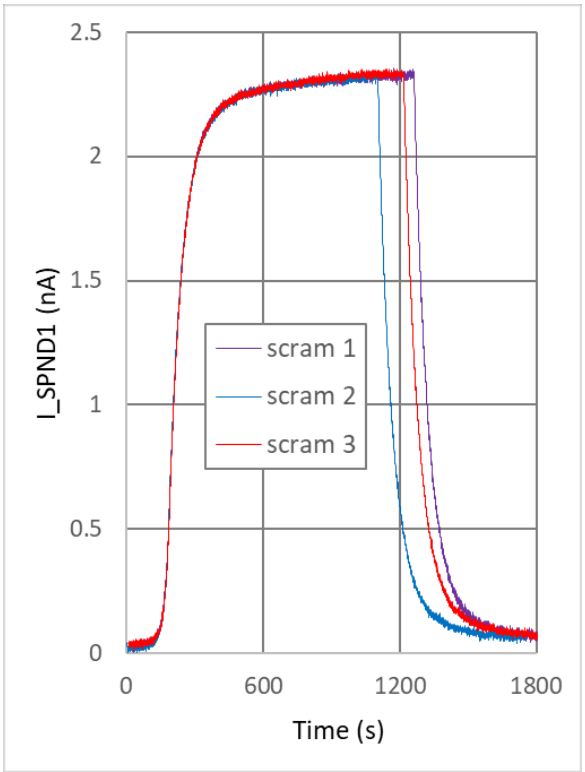

Fig. 7 – Three examples of differential signals (emitter minus compensator) of the SPND1 with BR1 operating at 300 kW followed by scram. Apart from the slightly different power-on time in the three cases, all three curves are nearly coinciding.

B. Comparison between signals of all SPNDs

The recorded signals of all seven SPNDs were compared with their average value. The percentage deviations were found to be:

- SPND1: +0.2%
- SPND2: -1.0%
- SPND3: -0.4%
- SPND4: +0.9%
- SPND5: +0.2%
- SPND6: +0.2%
- SPND7: -0.1%

So all signals are coherent within a margin of 1%. The flux gradients are expected to be smaller than 1%, but they are not known more accurately; so part of the differences between the SPND signals could even be due to flux gradients. The sensitivity dispersion between the seven SPNDs is within 1%.

C. Linearity

Figure 8 shows the average recorded net SPND currents (emitter currents minus compensator wire currents) as a function of the BR1 reactor power as deduced from the count rate of the reactor power monitoring fission chamber, from startup to the 1000 kW level. The deviations from a linear relation are within the combined uncertainty of the power determination (statistical uncertainty on the fission chamber count rate) and of the SPND current. This proves the proper functioning of the SPNDs in the complete range studied, from $0.8 \cdot 10^9$ n/(cm s) to $2.6 \cdot 10^{11}$ n/(cm s). It should be noted that the studied SPNDs gave already a readily measurable signal for a thermal neutron flux smaller than 10^9 n/(cm s).

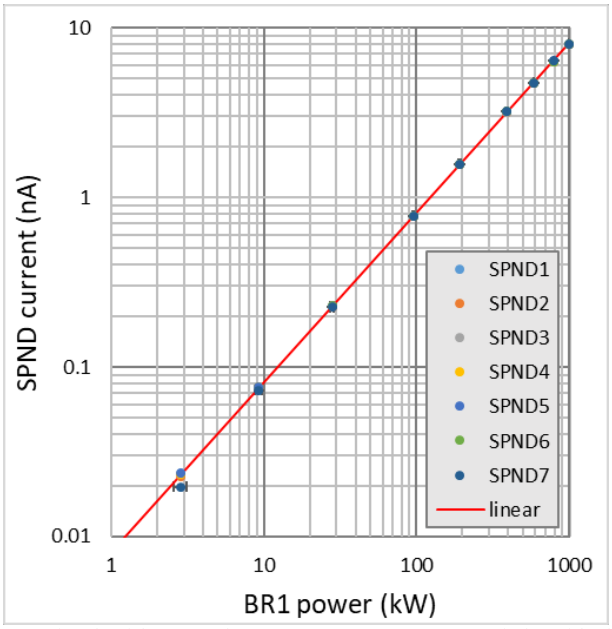

Fig. 8 – Signals of the 7 tested SPNDs vs. BR1 reactor power (in logarithmic scale). For one data set, all horizontal and vertical error bars are plotted; apart from the lowest flux point, all error bars fall within the dimensions of the data points, and the deviation from linearity is also less than these dimensions.

D. Reproducibility

Some test conditions were repeated several times in order to verify the reproducibility of the SPND response. As illustrated in Fig. 7, the obtained signals were very coherent, with mutual deviations below the 1% level.

E. Prompt signal component analysis

The distinction between the prompt and delayed components can be made in the clearest way by analyzing the scram data taken in fast acquisition mode, combining a high acquisition rate with a fast flux change. Fig. 9 shows part of the experimental data of Fig. 7, analyzed as a sum of a prompt component and a rhodium beta component. The relative prompt fractions deduced from the data of three subsequent tests are 4.0%, 4.1% and 4.0%, so on average 4.0%, which is somewhat lower than the 5.3% obtained by MCNP calculations (see Section 4). In the analysis of the slow acquisition data we will keep this ratio fixed at 4.0% for all seven SPNDs.

F. Analysis of the delayed signal components

In the slow acquisition rate data, the small contribution due to aluminum betas cannot be reliably disentangled from the rhodium beta contribution (similar characteristic time). Therefore, the calculated partial aluminum beta current of 5 pA

(for 700 kW reactor power) was applied in the analyses, in which the rhodium beta sensitivity and the manganese beta sensitivity were left as free parameters. The average equilibrium rhodium beta related current (normalized to 700 kW reactor power) was found to equal 5.21 nA and the average equilibrium manganese beta related current -9.0 pA. The dispersion between the rhodium beta currents in the different SPNDs was limited to 1%, while the individual manganese beta current values obtained for the different SPNDs ranged from -8.8±0.7 to -9.6±0.7 pA. Fig. 10 illustrates the analysis for the data of Fig. 6, averaged over all seven SPNDs.

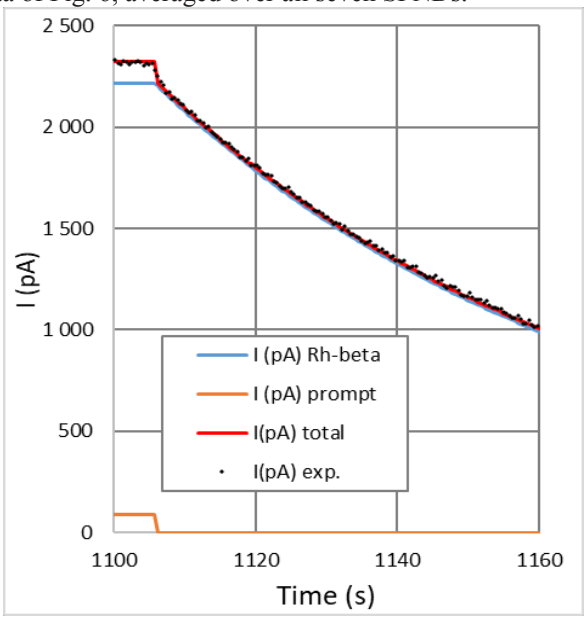

Fig. 9 –Analysis of the data of Fig. 7 in terms of prompt and rhodium beta contributions.

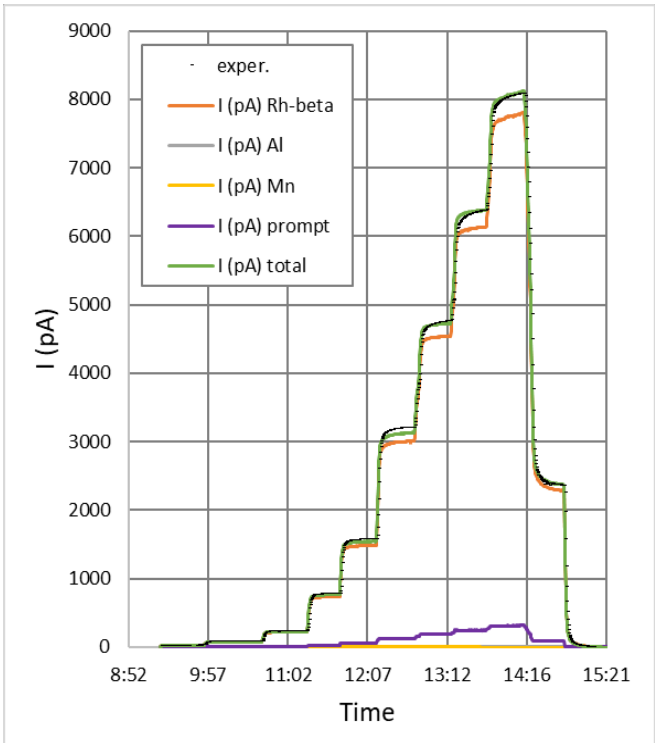

Fig. 10–Analysis of the data of Fig. 6 in terms of prompt and rhodium beta contributions.

VI. COMPARISON BETWEEN EXPERIMENTAL AND MCNP DATA

Table I summarizes the experimental and calculated partial current contributions, normalized to a reactor power of 700 kW. The total current and the rhodium beta related current values from experiment and calculations agree within 1%. The calculated total prompt current amounts to 0.31 nA, of which the majority (0.29 nA) would be due to neutrons and only 0.023 nA due to gammas. This value is significantly higher than the observed value of 0.22 nA (4.0% of the total current). The manganese beta related current is small and negative; the experimental and calculated values agree within the experimental uncertainty. The observed total current differs by only 1 % from the calculated value.

TABLE I
Experimental and calculated partial SPND currents and the percentage differences

	Exper.	Calc.	Rel. diff.
Rh beta	5.21 nA	5.18 nA	0.6 %
Mn beta	-0.009 nA	-0.0095 nA	5 %
Total prompt	0.22 nA	0.31 nA	29 %
Total	5.43 nA	5.49 nA	1 %

VII. CONCLUSIONS

Seven Thermocoax rhodium SPNDs from different fabrication batches were tested under irradiation in the BR1 reactor. The SPND signals were recorded during stepwise power-up of the reactor, proving the linearity of the SPND response down to a thermal neutron flux level below 10^9 n/(cm s). Intercomparison of the SPND signals showed a very small spread, confirming the repeatability of the fabrication process. The data were analyzed in terms of prompt and various delayed responses and the partial sensitivities were compared with theoretical sensitivities based on MCNP calculations. For the overall SPND neutron sensitivity an agreement within a 1% margin was achieved.

REFERENCES

1. M. Giot, L.Vermeeren, A. Lyoussi, C. Reynard-Carette, C. Lhuillier, P. Mégret, F. Deconinck and B. Soares Gonçalves, EPJ Nuclear Sci. Technol. 3, 33 (2017)

2. E. Malambu, "Characterization of neutron fields in support of dosimetry measurements in the BR1 reactor using MCNP/S code simulations", SCK•CEN Internal Report SCK•CEN-IR-182 (2010)

3. L. Vermeeren, IEEE Conf. Proc. 4th Intl. Conf. on Advancements in Nuclear Instrumentation Measurement Methods and their Applications (ANIMMA), IEEE Xplore (2016); doi: 10.1109/ANIMMA.2015.7465531